Design of Compensation Topologies for Wire-Less Power Transfer using Matlab

[1]B.Somashekar, [2]Dr.Ganapathy D Moger
[1]Research Scholar, East Point College of Engineering & Technology, Bangalore
& Associate Professor, Dr.T.Thimmaiah Institute of Technology, KGF
[2]Research Guide, EPCET, Bangalore

Abstract—Wireless power transmission devices are growing in acceptance and usefulness. This paper will discuss, examine, and contrast various compensation topologies for the transfer of inductive power. The classification of topology is changed. The difficulties of the five primary topological needs, standards, safety, and the physical underpinnings of compensatory labour are given considerable emphasis. The IPT is found to favour topologies with series main compensating over the four conventional systems for charging devices.

If the output voltage is low, the series-parallel method is preferable since it allows for the smallest possible size of the secondary side coil. The resonance load and the magnetic coupling coefficient frequency have no effect on the series-series solution. The comparative results are given in tables, graphs, and dependencies for ease of display and understanding utilizingmatlab programming and matlabsimlink.

Each application has its own set of core topologies. The main advantage of this research is that the results may be used as a "one-stop" information source and a selection guide for compensating topologies in terms of devices and power level. The literature study and current market developments for wireless power transmission devices highlight the main potential directions for evolving topologies.

Index Terms—WPT, IPT, compensation topology, requirement, Classification

I. INTRODUCTION

The governments of several nations promote research into alternative energy sources and electric vehicles as a plan for future technological

advancement. Therefore, the well-known benefits of wireless communication over connectors for power transfer and information transmission between devices are also being actively developed.

The capacitive and inductive methods of Wireless Power Transfer (WPT) have the most useful applications. The simplicity of setup, convenience of use, great efficiency at close range, and assurance of safety are further benefits of magnetic inductive coupling.

Consequently, industrial and mass-market distribution An inductive approach and an inductive method with resonance as its type have proven successful, particularly in the high-power applications.

The high-frequency inverter is where the grid's electricity is transformed into alternating current through the primary rectifier. The energy is transferred from the primary side of the device to the other side (secondary side) through a primary resonant circuit Cp-Lp with magnetically coupled coils. After being rectified, filtered, and sent to the load (RL), the resultant current.

A near-eld Electromagnetic Field (EMF) is employed in the WPT using electromagnetic induction. According to Ampre's law and Faraday's law, the alternating high-frequency electric current passing through the primary winding induces an alternating magnetic field that operates on the secondary winding. This phenomenon is known as electrodynamic induction. The interaction needs to be sufficiently close to attain high efficiency. The majority of the magnetic field does not reach the secondary winding when the secondary winding is separated from the primary, and as a result of the losses, the inductive coupling loses effectiveness.

As compared to IPT with the resonance, systems with merely inductive coupling are substantially less efficient. the leaking of the low and is made worse by the transformer's wide air gap.

Leading to a greater leakage inductance than with conventional transformers as a result. In general, the effectiveness of IPT without pay does not surpass 50%.

Reactive power on the primary and secondary sides, along with additional compensating capacitors, is needed to make up for the leakage

inductance.

The efficiency of the delivered power reduces more quickly as the distance between the coils grows as a result.

In a later section of this paper, the IPT with compensating circuits (also known as an inductive power transfer system with resonance) will be explained.

To guide the flow and increase coupling efficiency, the conductors are coiled on the magnetic conductive material. N_1, N_2 are the primary and secondary sides' respective turn counts; I_1, V_1, I_2, V_2 are the primary and secondary sides' current and voltage; C_1, C_2 are compensating resonant capacitors; and R are the load resistance and magnetic flux.

II. CLASSIFICATION OF DIFFERENT TOPOLOGIES

A topology with at least one resonant element on one side can be thought of as the compensation for an inductive energy transfer.

1. Location
   - One sided
     - Simple S & P
   - Multi sided
     - Modified
     - Complicated
   - Double sided
     - SP
     - SS
     - PS
     - PP
2. Number of Resonant Elements :
     - One or more

According to the position, the topologies are proposed to be classified. One, two, or more resonant elements may be present on each side. These could be inductors and capacitors. When using several coils, the compensating element or elements may be placed close to each coil, either exclusively on the transmitting or receiving side, or even on both.

III. ANALYSIS OF 4 BASIC COMPENSATION TOPOLOGIES

As illustrated in the figure, there are 4 main compensatory topologies on which most semiconductor solutions are based: Serial-Serial (SS), Serial-Parallel (SP), Parallel-Serial (PS), and Parallel-Parallel (PP) are the four types of parallel processing.

WPT research was done a very long time ago, but more recently, since the 1990s has been dedicated to IPT systems with compensation.

Electric car and mobile phone markets were just getting started at the time. Initially, several formulae were without taking specific process parameters into account, is used to calculate the principal compensating capacityand specifications. Some designs compute primary capacitance by just correcting for primary self-inductance. If the reactive impedance is minimal in relation to the primary self-inductance, this is acceptable. Furthermore, bifurcation-free functioning is commonly expected.

Initially, only solely inductive WPT systems for charging electric vehicles were studied.

A well-known study at the Massachusetts Institute of Technology (MIT) in 2007 provided a significant impetus to the development of WPT with compensation. The MIT study team discovered that when gearbox coils act in resonance, the efficiency and transfer distance can increase

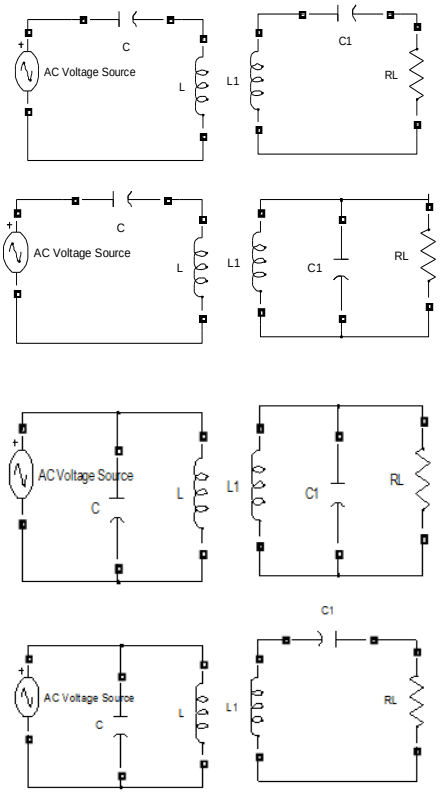

FIG 1 : DIFFERENT TOPOLOGIES

IV (A)ANALYSIS OF BASIC TOPOLOGIES

The characteristics of the fundamental compensation topologies must be carefully taken into account in order to be understood. The fundamental equations and the comparison's outcomes are displayed in the equations..

According to a detailed assessment of the fundamental compensation topologies offered, the choice of the L and C values of the resonant circle is mostly determined by the primary or secondary topology, the quality factor, and the magnitude of the magnetic coupling coefficient. By comparing the SS and SP parameters, it is clear that topology selection has a considerable impact on primary capacity selection.

According to Kirchhoff's voltage law, the mathematical equation of the SP model and the SS model can be established as equation.

$$us = Z_1 I_1 - jwMI_2 \qquad (1)$$
$$0 = jwmI_1 - I_2$$

Where Z_1 represents the transmitting circuit's impedance and Z_2 represents the receiving circuit's impedance,
$Z_r=\omega^2 M\, Z_2$ is the reflected impedance, The mutual inductance of the transmitting and receiving coils is denoted by M.Take SP model as a example to analyze, the impedances in equation (1) can be obtained as equation (2)

$$z_{1=R_S} + j\omega L_1 + \frac{1}{j\omega C_1}$$
$$Z_2 = j\omega L_2 + \frac{1}{j\omega C_2} + \frac{1}{R_L} \qquad (2)$$

Most designers used the inductances L1=L2=L, compensatory capacitances C1=C2=C, and the angular frequency of the driving source is ω0 =1 / *LC* .while designing the magnetically coupled resonant WPT system. The transmitting circuit and receiving circuit are not in the resonant situation because the magnetically linked resonant WPT system is not in the magnetically coupled resonant situation.

In other words, rather than just choosing L1=L2=L and C1=C2=C, another approach should be employed to design the inductance or compensatory capacitances to produce the WPT system in a magnetically coupled resonant scenario.
Based on the preceding analysis, a solution to this problem is offered, and the processing mechanism is as follows: (1) the structures and parameters of the transmitting and receiving coils are identical, which means $L_1 = L_2 = L$; (2) the compensating capacitance of the receiving coil C_2 is fixed, while that of the transmitting coil C_1 is adjustable; (3) the angular frequency of the system can be determined to ensure the resonant of the receiving circuit; and (4) the compensating capacitance C_1 can be determined based on the resonant angular frequency. Following the following steps, it is possible to assure that the WPT system distributes power wirelessly in a magnetically linked resonant condition.

The compensating capacitance C_1can be obtained as formula,

$$C_1 = {}^{1}/_{\omega_0^2} = \frac{C_2^2 R_L^2}{C_2 R_L^2 - L} \qquad (3)$$

So as $L_1=L_2=L$ and the compensating capacitance of receiving coil $C_2$is fixed, and the angular frequency ofdriving source is

$$\omega_0 = \sqrt{(c_2 R_L^2 - L)/(LC_2^2 R_L^2)} \qquad (4)$$, and the
compensating capacitance of transmitting coil is

$$C_1 = {}^{1}/_{\omega_0^2} = \frac{C_2^2 R_L^2}{C_2 R_L^2 - L} \qquad (5)$$

, the WPT system is magnetically coupled resonant, and the transfer power and efficiency is deduced as equation

$$P_{out} = U_S^2 \frac{\frac{\omega_0^2 M^2}{R_L}(1 + \omega_0^2 C_2^2 R_L^2)}{(R_S + \frac{\omega_0^2 M^2}{R_L}(1 + \omega_0^2 C_2^2 R_L^2))^2} \qquad (6)$$

$$\eta_{eff} = U_S^2 \frac{\frac{\omega_{0M}^2}{R_L}(1+\omega_0^2 C_2^2 R_L^2)}{R_S + \frac{\omega_0^2 M^2}{R_L}(1+\omega_0^2 C_2^2 R_L^2)} \qquad (7)$$

The same analysis procedure is used for the SS model and since C1=C2 is used as the compensatory capacitance, the transfer power and efficiency are determined.

$$P_{out} = U_S^2 \frac{\frac{\omega_{0M}^2}{R_L}}{(R_S + \frac{\omega_0^2 M^2}{R_L})^2} \qquad (8)$$

$$\eta_{eff} = \frac{\frac{\omega_{0M^2}^2}{R_L}}{R_S + \frac{\omega_{0}^2 M^2}{R_L}} \quad (9)$$

Z1 and Z2 have the following specific numerical values in equation for the PS model,

$z_{1=}j\omega L_1$

$$Z_2 = R_L + \frac{1}{j\omega C_2} + j\omega L_2 \quad (10)$$

And in equation, Z1 and Z2's precise numerical values for the PP model are as follows

$z_{1=}j\omega L_1$

$$Z_2 = \frac{R_L}{1 + \omega^2 C_2^2 R_L^2} + j\omega L_2 - j\omega C_2 \frac{R_L^2}{1 + \omega^2 C_2^2 R_L^2} \quad (11)$$

The transfer power and efficiency for PS model and PP model are derived as equation using the same analysis method as with SP model previously, which attempts to make the transmitting circuit and receiving circuit be pure resistive

$$P_{out} = U_S^2 \frac{\frac{\omega_{0M^2}^2}{R_L}}{\omega_{0}^2 L^2 + (\frac{\omega_{0}^2 M^2}{R_L})^2} \quad (12)$$

$$\eta_{eff} = \frac{\frac{\omega_{0M^2}^2}{R_L}}{\sqrt{\omega_{0}^2 L^2 + (\frac{\omega_{0}^2 M^2}{R_L})^2}} \quad (13)$$

$$P_{out} = U_S^2 \frac{\frac{\omega_{0M^2}^2}{R_L}(1+\omega_0^2 C_2^2 R_L^2)}{\omega_{0}^2 L^2 + (\frac{\omega_{0}^2 M^2}{R_L}(1+\omega_0^2 C_2^2 R_L^2)^2} \quad (14)$$

$$\eta_{eff} = \frac{\frac{\omega_{0M^2}^2}{R_L}(1+\omega_0^2 C_2^2 R_L^2)}{\sqrt{\omega_{0}^2 L^2 + \frac{\omega_{0}^2 M^2}{R_L}(1+\omega_0^2 C_2^2 R_L^2)}} \quad (15)$$

As Table I determines the compensating capacitances for transmitting coils and resonant angular frequency, Table II displays the reflected impedance Zr, impedance ZS, transfer power, and efficiency for each model.

Tabel-1 compensating capacitances for transmitting and resonant frequency for four modules

Modules	C_1 - compensating capacitances	ω_0 – Angular frequency
SS	C_2	$\sqrt{\frac{1}{LC_2}}$
SP	$C_2\left(1 + \frac{L}{-L + C_2R_L^2}\right)$	$\sqrt{\frac{1}{LC_2} - \frac{1}{R_L^2C_2^2}}$
PS	$\frac{C_2^2L^3}{C_2^2L^3 + \frac{M^4}{R_L^2}}$	$\sqrt{\frac{1}{LC_2}}$
P	$\frac{C_2^2L^5}{C_2L^5 - \frac{L^5}{R_L^2} + \frac{M^2}{R_L^2}(C_2R}$	$\sqrt{\frac{1}{LC_2} - \frac{1}{R_L^2C_2^2}}$

Tabel-2 Reflected Impedance, Transfer Power and Efficiency

Modules	Reflected Impedance	Impedance	Transfer Power	Transfer Efficiency
SS	$\frac{M^2\omega_0^2}{R_L}$	R_S	$U_S^2\frac{Z}{(Z_S +$	$\frac{Z_R}{Z_S + Z_R}$
SP	$\frac{\omega_0^2M^2}{R_L}(1$ $+ \omega_0^2C_2^2R$	R_S	$U_S^2\frac{Z}{(Z_S +$	$\frac{Z_R}{Z_S + Z_R}$
PS	$\frac{M^2\omega_0^2}{R_L}$	$\sqrt{\frac{1}{LC_2}}$	$U_S^2\frac{Z}{(Z_S^2 +$	$\frac{Z_R}{\sqrt{Z_S^2 + Z_R^2}}$

IV (B)MODIFICATION AND COMBINATION OF COMPENSATION TOPOLOGIES

They may consist of additional inductances in series or parallel, or combinations of 2 or more capacitors on one side. There are additional capacitance&inductance (C and L) pairings for parallel connections.

Across their entire coupling and loading range, the hybrid topologies (LCL-LCL and LCC-LCC) maintain high efficiency. However, hybrid topologies may result in significantly higher copper loss than SS topologies under rated power, particularly when transmitting high power, due to the additional inductances and capacitances as well as associated stray resistances. Compared to SS topologies, hybrid topologies have more control complexity and cost. Despite this, when combined with a voltage source inverter on the primary side, the secondary side current source behaviours of the LCL-LCL and LCC-LCC topologies make them appropriate forbattery-charging applications. A capacitor and an inductor have opposite-phase equivalent impedances. The t circuit in hybrid circuits for large electric bicycle charging can be built with either the LCL or CLC architecture.

The RMS output current of the double-sided LCC compensation architecture is constant once the input voltage is fixed. It is possible to achieve Zero Current Switching (ZCS) by fine-tuning the LCC compensation. In order to provide a pickup with a unity power factor, the LCC pickup can also compensate for reactive power on the secondary side. This compensation is independent of the coupling coefficient and the load conditions. The most common is double-sided LCC compensation, which has great efficiency, misalignment tolerance, and load independence qualities and may lower current stress in the inverter.

Either the parallel or series nature of the secondary side of the LCC compensation is possible. Because it resists changes in load, parallel compensation is often used. The transferred-impedance on the primary side of the parallel tuned system, which comprises both real and fictitious load components, is a drawback. The series tuned pickup needs a large bridge rectifier capacitor to maintain continuous conduction, and at high power levels, the pickup voltage increases to a high value.

The foregoing problems are resolved by the LCC topology, which also offers the advantages listed below: Higher system efficiency compared to parallel pickup; lower losses in the rectifier and pickup winding. The advantages of the series primary resonant circuit include a constant supply voltage and the series capacitor's ability to block the dc component from the input voltage. On the other hand, a large, high-frequency current will be passed through a series capacitor to produce the high capacitor voltage. The parallel primary circuit has dc component blocking but offers constant supply current and no load management. While only reflecting a genuine portion of the resistance to the primary side, the series secondary resonant circuit on the secondary side produces stable voltage.
The parallel secondary resonant circuit provides a stable current suitable for charging batteries. This circuit's primary side can detect both actual and fictitious impedances. The resonance frequency fluctuates as the load varies. In reality, the secondary load cannot be modeled as a nonlinear load and pure resistance, which raises the system order. In an effort to combine the benefits of both straightforward resonant circuits, the LCL-LCCL resonant circuit is described. The huge volume of a dual side LCC compensating is a drawback. A hybrid compensation topology that combines series compensation and LCC compensation with two extra switches is employed for the receiver and transmitter sides.

High-order compensation topologies like the LCC and LCL are becoming more popular because to their higher overall performance. Inverters with double-sided LCC resonant design are frequently controlled at a set frequency. As a result, an auxiliary switching power a converter is required to control the output power

V.MAT LAB PROGRAMMING

By applying the equation mentioned in the aforementioned article and the input data, a matlab code is built to determine the transfer power and efficiency for various topologies. The results of several topologies, including Series Series , Series Parallel, Parallel Parallel, and Parallel Series , are reported.

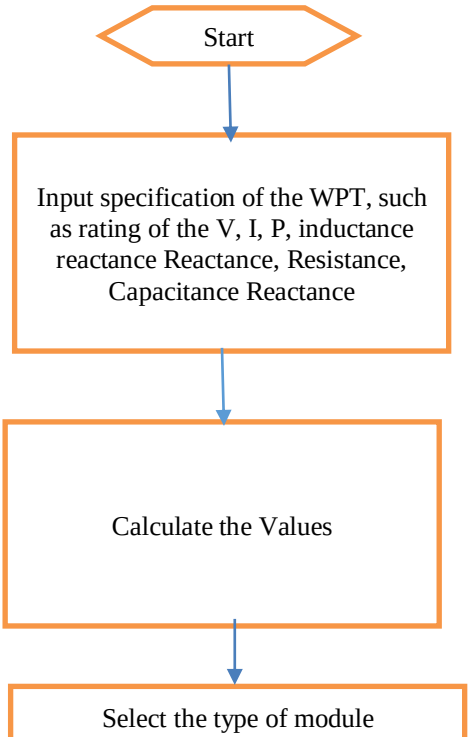

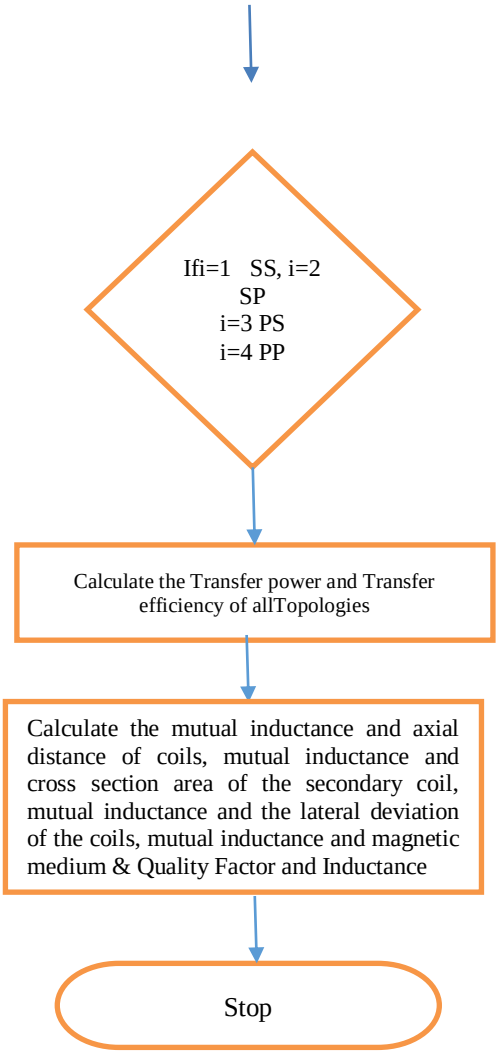

Fig 2 Flow chart of matlab programming

Input Specification of the Mat lab Program

L_1=29.6e-6 Henry
R_s=50 Ohms
R_L=50 Ohms
C_2=2.28e-6 Farad
K=0.075

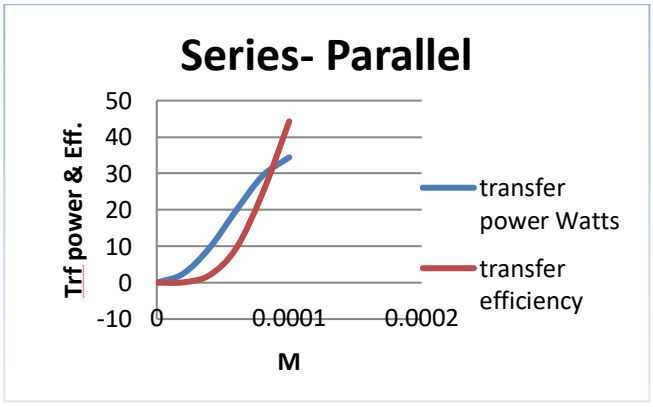

Fig 3: Mutual Inductance vs Transfer Power, Transfer Efficiency

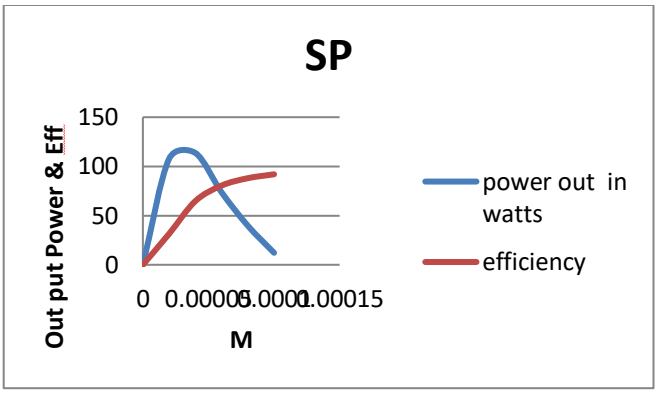

Fig 4: Mutual Inductance vs Output Power, Efficiency

Series parallel topologies mean that the transmitter side capacitor is connected in series and the receiver side capacitor is connected in parallel, the C1 is fixed where as C2 is calculated from the program and results are tabulated, from the results plotted in the graph as shown in fig 3, as the mutual inductance increases the transfer power and transfer efficiency increases, the maximum transfer efficiency is around 44.29% for a.Micro Henery and from the fig 4 displayed reveals that when the mutual inductance grows, the output efficiency also increases. For a value of M is 0.001Micro hennery, the efficiency is 91.98, while the output power reduces to 12.19 Watts.

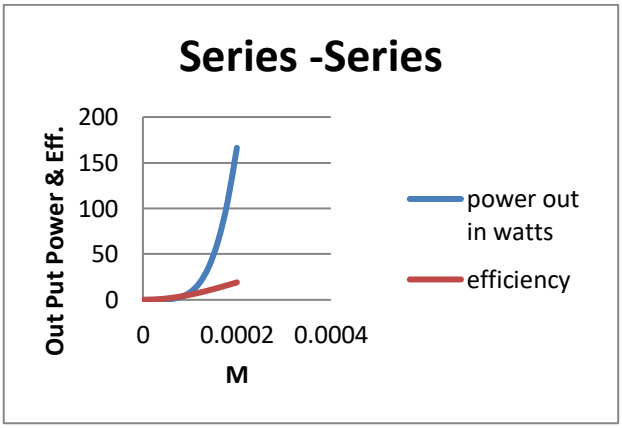

Fig 5: Mutual Inductance vs Transfer power, Efficiency

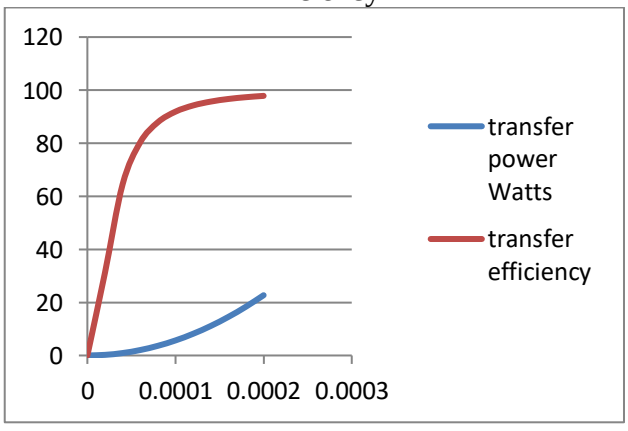

Fig 6: Mutual Inductance vs Output Power, Efficiency

Series topologies mean that the transmitter side capacitor is connected in series and the receiver side capacitor is connected in series, the C1 is fixed where as C2 is calculated from the program and results are tabulated, the results are plotted in the graph as shown in fig 5, as the mutual inductance increases the output power and output efficiency, the maximum output efficiency is around 19.08% for a value of M. and from the fig 6 displayed reveals that as the mutual inductance grows, the transfer efficiency also increases. For a value of M is 0.002 micro hennery, the efficiency is 97.84, while the transfer power reduces to a value of 22.708Watts.

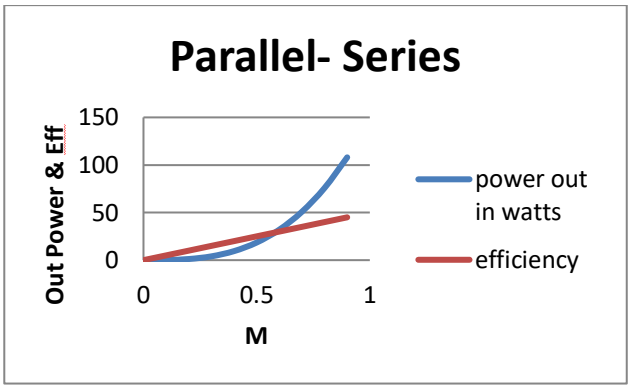

Fig 7: Mutual Inductance vs. out power, Efficiency

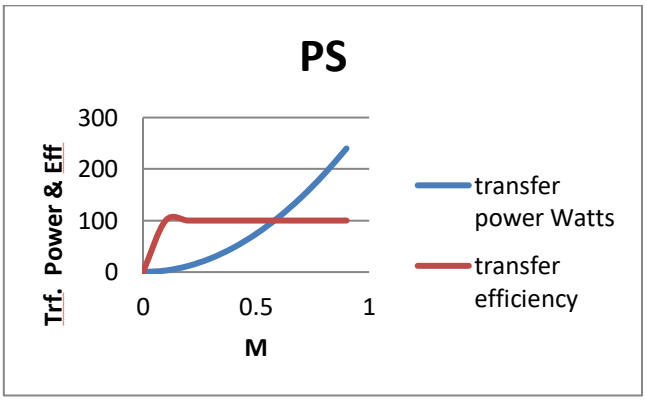

Fig 8: Mutual Inductance vs. Output Power, Efficiency

Parallel-Series topologies mean that the transmitter side capacitor is connected in parallel and the receiver side capacitor is connected in series, the C1 is fixed where as C2 is calculated from the program and results are tabulated, the results are plotted in the graph as shown in fig 7, as the mutual inductance increases the transfer power and transfer efficiency, the maximum transfer efficiency is around 19.08% and from fig 8 displayed reveals that as the mutual inductance grows, the transfer efficiency also increases. For a value of M is 0.900001 Micro hennery, the efficiency is 100, while the transfer power reduces to 240.04 Watts.

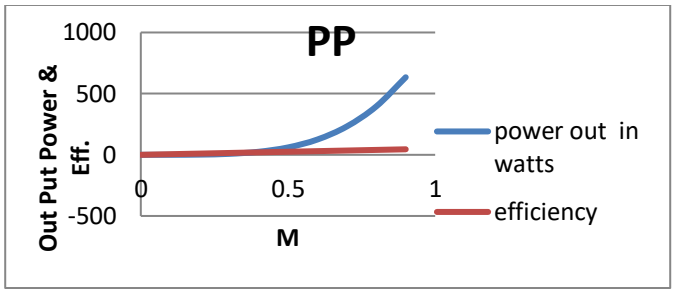

Fig 9: Mutual Inductance vs. Output Power, Efficiency

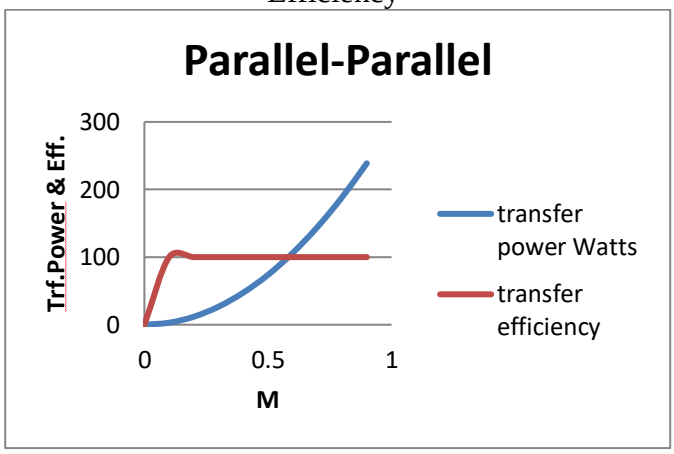

Fig 10: Mutual Inductance vs. Transfer Power, Efficiency

The results are tabulated, and the results are plotted on the graph as shown in fig. 9. This means that in a parallel topology, the transmitter side capacitor and the receiver side capacitor are connected in parallel. The maximum transfer efficiency is approximately 45% for a value of M of 0.900001 Micro Henery, and the output power is approximately 633.8 watts. C1 is fixed, while C2 is calculated from the program. Additionally, the plotted data in Figure 10 indicates that when mutual inductance rises, transfer efficiency rises as well. For example, at a value of M of 0.900001 Micro Henery, the efficiency is 100, while the transfer power falls to a value of 238.79 Watts.

Table 3 shows the results of computing the relationship between mutual inductance and axial distance using the formula

$$M = (39 * 1^{-0.073*d}) + (12 * 1^{-0.017*d})10^{-6}$$

Table 3: The relation between mutual inductance and axial distance of coils

D Cms	M Micro Henry
0	0
0.5	19.5
1	39
1.5	585
2	78
2.5	97

3	117
3.5	136.5
4	156
4.5	175
5	195

the relationship between mutual inductance and axial distance between the transmitter and receiver yields the following results: for a distance of 5 cms, the value of M is 195 Micro hennery, and the mutual inductance increases as the distance between the transmitter and receiver increases. These results are obtained from the matlab programming.

The results of applying the formula to determine the relationship between mutual inductance and secondary coil cross section area are shown in Table 4.

$$M = \frac{20s^2 - 26 * s + 21}{(100s^2 - 150s + 120\,)10^{-6}}$$

Table 4: The relation between mutual inductance and cross section area of the secondary coil

S in Sq Cms	M
0	0.175
10	0.204292
20	0.202074
30	0.201367
40	0.201019
50	0.200812
60	0.200675
70	0.200578
80	0.200505
90	0.200448
100	0.200403

Table 4 present the results of the Mat Lab programming for the relationship between mutual inductance and the secondary coil's cross section area. The analysis of the graph indicates that, as the secondary side's cross-section area increases, the mutual inductance stays constant, reaching a value of 0.204292 micro hennery at a distance of 10 Sq Cms.

The mutual inductance and coil lateral deviation calculations are shown in Table 5 using the formula.

$$M = \frac{40g + 810}{(g + 19)10^{-6}}$$

Table 5: The relation between mutual inductance and the lateral deviation of the coils

G in cms	M
0	0.000043
1	0.000039
2	0.000035
3	0.000031
4	0.000028
5	0.000025
6	0.000023
7	0.00002
8	0.000018
9	0.000016
10	0.000014
11	0.000012

Using the formula, Table 6 displays mutual inductance and the magnetic medium.

$$M = \frac{36\,w_1^2 - 385w - 83}{(w_1^2 - 11w_1 - 3\,)10^{-6}}$$

Table 6: The relation between mutual inductance and magnetic medium

w1	M Micro Henry
0	15.621652
1	3.604994
2	2.231658
3	1.735727
4	1.511754
5	1.420123
6	1.420111
7	1.511716
8	1.735654
9	2.231526
10	3.60472
11	15.6202
12	5.206641

A graph is created using Mat lab code. Figure 11 demonstrates the relationship between quality factor and inductance using the formula.

the graph in fig.11 depicts the relationship between inductance and the quality factor based on the findings obtained from the mat lab code. as the inductance of L_1 and L_2 increases, so do the quality factors of Q_1 and Q_2

$$w_0 = 2 * 3.14 * f$$
$$L_1 = \frac{Q_1 \, r_1}{w_0}$$
$$L_2 = \frac{Q_2 \, r_2}{w_0}$$

Quality Factor and Inductance

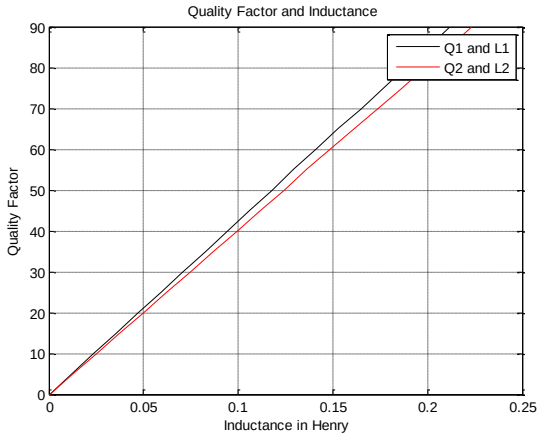

Fig 11: Quality Factor and Inductance

VI. MAT LAB SIMULATION

Mat lab simulation was performed using computed values from the mat lab programming. The results and graphs are displayed in the figures below, and the results are compared to the code values. Different topologies, including parallel-series, parallel-parallel, series-parallel, and series-parallel combination, are all used in the simulation.

The rectifier device converts the 230V, 50 Hz AC voltage in the simulation circuit to DC and is connected to the IGBT circuit via an RC filter that filters harmonics. IGBT power modules are used in IGBT inverters to ensure high voltage/power switching capabilities. The IGBT inverter serves as the brain of the electric drive system. The "heart" of the electrified drive train is thought to be the IGBT power module. The WPT (Mutual Inductance) receives the output voltage from the IGBT, which is then fed to the rectifier unit, which transforms the output voltage from the rectifier unit to the DC, the output voltage is fed to the battery charging device, which charges to the rated voltage value. The charge that is kept at its nominal value of 230 DC and is used to power the electric vehicle.

Series Series Model:

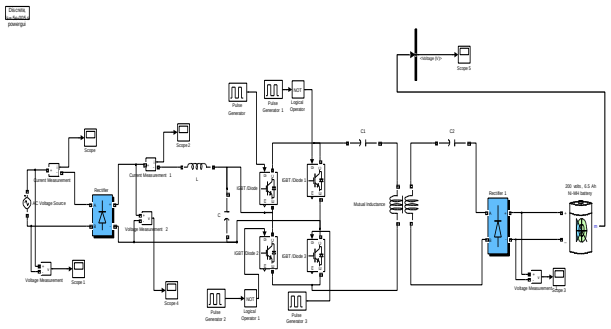

Fig 12: Series–Series Simulation Model

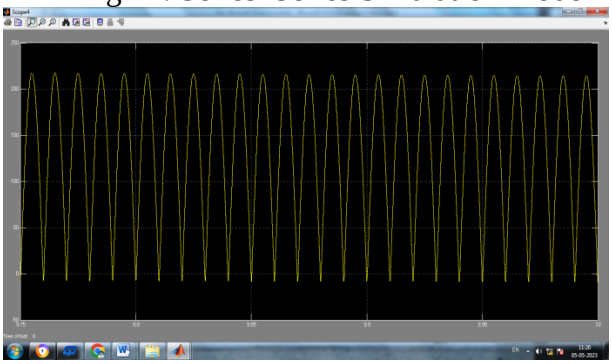

Fig 13: SS Rectified Out Put

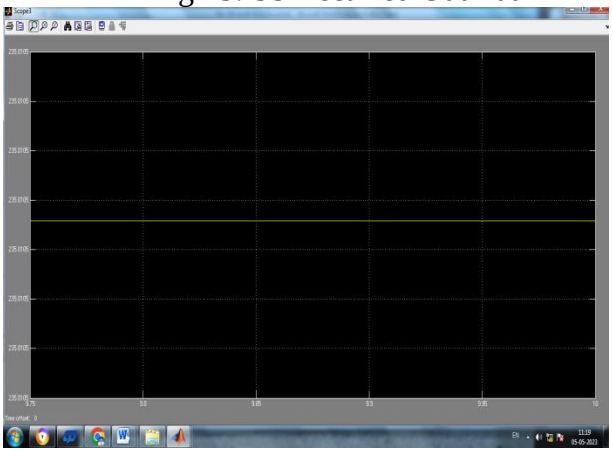

Fig 14: SS- Battery Charging Voltage

Series Parallel Model:

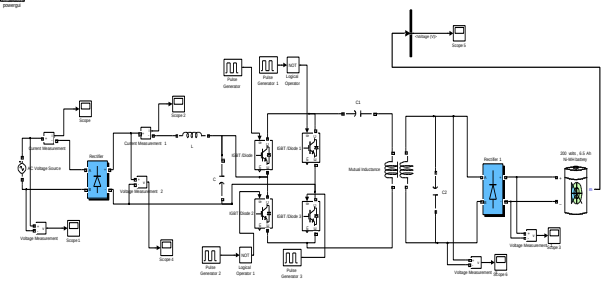

Fig 15: Series–Parallel Simulation Model

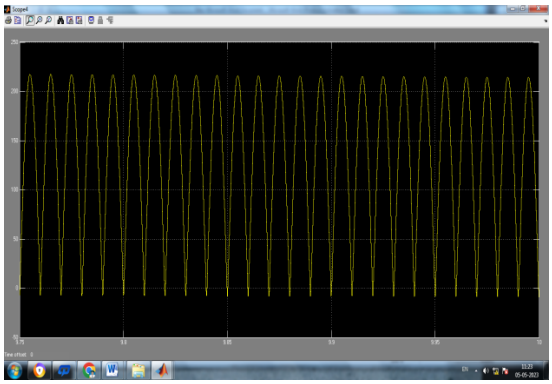

Fig 16: SP Rectified Out Put

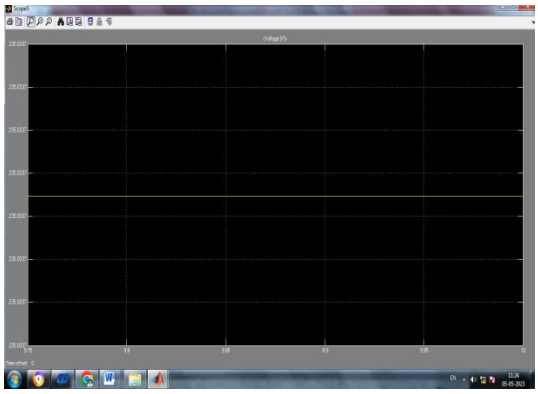

Fig 17: SP- Battery Charging Voltage

Parallel Series Model

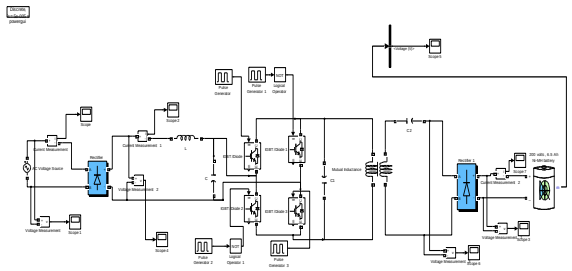

Fig 18: Parallel- Series Simulation Model

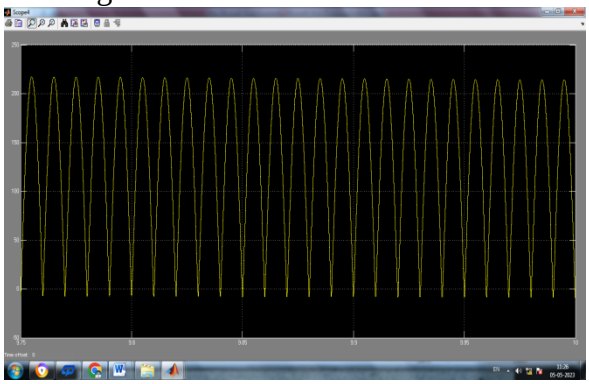

Fig 19: PS Rectified Out Put

Fig 20: PS- Battery Charging Voltage

Parallel Parallel Model:

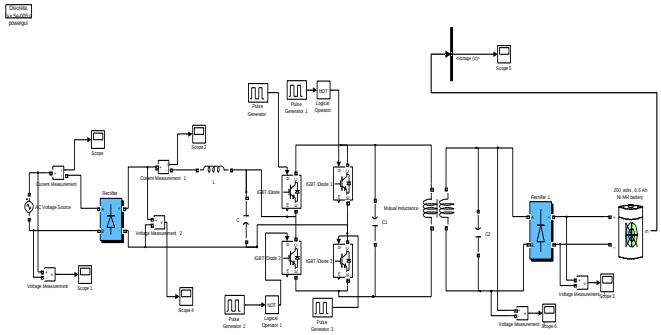

Fig 21: Parallel - Parallel Simulation Model

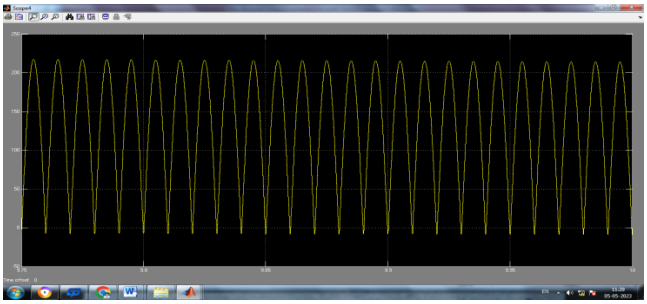

Fig 22: PS Rectified Out Put

Fig 23: PS- Battery Charging Voltage

TABLE 7: COMPARISON OF RESULTS OF DIFFERENT TOPOLOGIES

Topologies	Input Voltage	Rectified Voltage	Battery Charging Voltage
SS	230	217.4	235.1
SP	230	217.4	235
PS	230	217.3	235
PP	230	217	242.8

According to the table, the battery charging voltage is higher than the input voltage and rectified voltage because of the IGBT, which raises the output voltage.

SIMULATION RESULTS:

Using the simulation experiment feature of the software Matlab Simlink, it is further shown that the PP model is the best structure for a relatively long-distance WPT system in terms of transfer power and efficiency. All of the simulation experiment's parameters, including L1=L2=29.6H, C2=2.28F, RS=50 ohms, and RL=50 ohms, are taken from references as in [21] and [22] to

guarantee its dependability and availability. The mutual inductance of two coils decreases with increasing distance between them, according to the prior studies. Additionally, because $M = k\sqrt{L_1 L_{21}}$ and coupling coefficient k are proportional to mutual inductance, a smaller coupling coefficient k indicates a longer transfer distance. For a further analysis, it It is possible to determine that 0–0.1 is the ideal range for choosing coupling coefficient k. It is explained by the simulation findings for k=0.075, which compare the transfer powers and efficiency of four models.

The PP model transfers far more power from the simulation than the other models and it does so with the highest efficiency of the four models. Since the PP model has the best performance in terms of efficiency and power transfer, it is evident that it is the best option for building a resonant WPT system. And these results of the previous analysis agree with this.

VII. CONCLUSION

IPT systems are gaining popularity in research, particularly in Charging a battery wirelessly applications. This study provides a complete analytical review of compensation topologies in the IPT.

This research focuses on the various types of compensation circuits and how they are produced. The most efficient topologies in the IPT for charging devices have substantial compensating capacitors in series, with up to 97% efficiency, out of the 4 classical schemes. For most applications and power levels, it has been established that the Series-Series and Series-Parallel topologies will be the most optimal for most of the parameters among all topologies. For the unit turns ratio between the primary and secondary coils, the SS topology is recommended. The resonance frequency's load or magnetic coupling coefficients have no impact on it. Simultaneously, the SP solution is advised in the event of a low output voltage. The secondary side coil can be made as small as possible, however the primary side requires additional tuning in the event of distance change.

We can create the Compensation topologies that use a parallel primary connection are only appropriate for high-power applications. The combination of the LCC and LCL in WPT systems is superior to others with modified topologies, with more efficiency at a specific operation point. The basic purpose of developing compensating topologies is to increase the frequency of the resonant link. The development of novel high-frequency magnetic and semiconductor materials with improved characteristics will be prioritized.

REFERENCES

[1] C. Xia, Y. Zhou, J. Zhang, and C. Li, ``Comparison of power transfercharacteristics between CPT and IPT system and mutual inductanceoptimization for IPT system," J. Comput., vol. 7, no. 11, pp. 2734_2741,2012.

[2] F. MusaviandW.Eberle, ``Overview of wireless power transfer technologiesfor electric vehicle battery charging," IET Power Electron., vol. 7,no. 1, pp. 60_66, Jan. 2014.

[3] I. Korotyeyev, I. V. Pentegov, R. Strzelecki, and I. V. Volkov, ``Badanie procesówtesli w wybranychuk[a]adachprostownikowych," in Proc. PodstawoweProblemyEnergoelektronikiElektromechaniki (PPEE), Materia[a]y Sympozjum, Wis[a]a, Polska, 2000, pp. 375_378.

[4] X. Lu, P. Wang, D. Niyato, D. I. Kim, and Z. Han, ``Wireless charging technologies: Fundamentals, standards, and network applications," IEEE Commun. Surveys Tuts., vol. 18, no. 2, pp. 1413_1452, 2nd Quart., 2016.

[5] J. D. Jackson, Classical Electrodynamics, 3rd ed. New York, NY, USA: Wiley, 1999.

[6] M. H. Ameri, A. Y. Varjani, and M. Mohamadian, ``A new maximum inductive power transmission capacity tracking method," J. Power Electron., vol. 16, no. 6, pp. 2202_2211, Nov. 2016.

[7] D. Patil, M. K. McDonough, J. M. Miller, B. Fahimi, and P. T. Balsara, ``Wireless power transfer for vehicular applications: Overview and challenges," IEEE Trans. Transport. Electri_c., vol. 4, no. 1, pp. 3_37, Mar. 2018.

[8] Z. U. Zahid, C. Zheng, R. Chen, W. E. Faraci, J.-S. J. Lai, M. Senesky, and D. Anderson, ``Design and control of a single-stage large air-gapped transformer isolated battery charger for wide-range output voltage for EV applications," in Proc. IEEE Energy Convers. Congr.Expo., Denver, CO, USA, Sep. 2013, pp. 5481_5487.

[9] B. L. Cannon, J. F. Hoburg, D. D. Stancil, and S. C. Goldstein, ``Magnetic resonant coupling as a potential means for wireless power transfer to multiple small receivers," IEEE Trans. Power Electron., vol. 24, no. 7, pp. 1819_1825, Jul. 2009.

[10] W. Zhang and C. C. Mi, ``Compensation topologies of high-power wireless power transfer systems," IEEE Trans. Veh. Technol., vol. 65, no. 6, pp. 4768_4778, Jun. 2015.

[11] T. Kan, T.-D. Nguyen, J. C. White, R. K. Malhan, and C. C. Mi, ``A new integration technique for an electric vehicle wireless charging system employing LCC compensation topology: Analysis and design, IEEE Trans. Power Electron., vol. 32, no. 2, pp. 1638_1650, February 2017.

[12] Wireless Power Transfer for Light-Duty lug-in/Electric Vehicles and Alignment Methodology, Standard J2954_201904, SAE, 2016. [Online]. Available: http://standards.sae.org/wip/j2954/

[13] D. Kettles, Electric Vehicle Charging Technology Analysis And Standards, Standard FSEC-CR-1996-15, 2015. [Online]. Available: http://www.fsec.ucf.edu/en /publications/pdf/FSEC-CR-1996-15.pdf

[14] On-Line Electric Vehicle (OLEV) Project and Vehicular Wireless Power Transfer Technology. [Online]. Available: http://greentechlatvia.eu/wp-content/uploads/bsk-pdf-manager/2-5a_OLEV_Project_and_ Technology_(Ahn)_rev_a_15.pdf

[15] X. Lu, D. Niyato, P.Wang, D. I. Kim, and Z. Han, ``Wireless charger networking for mobile devices: Fundamentals, standards, and applications," IEEE Wireless Commun., vol. 22, no. 2, pp. 126_135, Apr. 2015.

[16] Qi [Electronic Resource]. Wireless Power Consortium.[Online]. Available: https://www.wirelesspowerconsortium.com
[17] K. Finkenzeller, RFID Handbook, 2nd ed. New York, NY, USA: Wiley, 2003, pp. 161_181.
[18] K. Tomita, R. Shinoda, T. Kuroda, and H. Ishikuro, ``1-W 3.3_16.3-V boosting wireless power transfer circuits with vector summing power controller," IEEE J. Solid-State Circuits, vol. 47, no. 11, pp. 2576_2585, Nov. 2012.
[19] M. A. Houran, X. Yang, and W. Chen, ``Magnetically coupled resonance WPT: Review of compensation topologies, resonator structures with misalignment,
and EMI diagnostics," Electronics, vol. 7, no. 11, p. 296, 2018.
[20] R. Tseng, B. von Novak, S. Shevde, and K. A. Grajski, ``Introduction to the alliance for wireless power loosely-coupled wireless power transfer system speci_cation version 1.0," in Proc. IEEE Wireless Power Transf. (WPT), Perugia, Italy, May 2013, pp. 79_83.
[21] C. T. Rim, Practical Design of Wireless Electric Vehicles: Dynamic & Stationary Charging Technologies. 2017.
[22] Review and Evaluation of Wireless Power Transfer (WPT) for Electric Transit Applications. [Online]. Available: https://www.transit.dot.gov/
sites/fta.dot.gov/_les/FTA_Report_No._0060.pdf
[23] International Commission on Non-Ionizing Radiation Protection, ``Guidelines for limiting exposure to time-varying electric and magnetic _elds (1 Hz to 100 kHz)," Health Phys., vol. 99, no. 6, pp. 818_836, 2010.
[24] M. Song, P. Belov, and P. Kapitanova, ``Wireless power transfer inspired by the modern trends in electromagnetics," Appl. Phys. Rev., vol. 4, no. 2, 2017, Art. no. 021102.
[25] IEEE Standard for MilitaryWorkplaces_Force Health Protection Regarding Personnel Exposure to Electric, Magnetic, and Electromagnetic Fields, 0 Hz to 300 GHz, IEEE Standard C95.1-2345, May 2014.
[26] K. Aditya and S. S. Williamson, ``Design considerations for looselycoupled inductive power transfer (IPT) system for electric vehicle battery
charging_A comprehensive review," in *Proc. IEEE Transp. Electri_c.Conf. Expo (ITEC)*, Dearborn, MI, USA, Jun. 2014, pp. 1_6.
[27] R. C. Fernandes and A. A. de Oliveira, ``Theoretical bifurcation boundaries
for Wireless Power Transfer converters," in *Proc. IEEE 13thBrazilian Power Electron. Conf. 1st Southern Power Electron. Conf.(COBEP/SPEC)*, Fortaleza, Brazil, Nov./Dec. 2015, pp. 1_4.
[28] C.-S. Wang, G. A. Covic, and O. H. Stielau, ``Power transfer capabilityand bifurcation phenomena of loosely coupled inductive power transfersystems," *IEEE Trans. Ind. Electron.*, vol. 51, no. 1, pp. 148_157,Feb. 2004.
[29] G. B. Joun and B. H. Cho, ``An energy transmission system for an arti_cialheart using leakage inductance compensation of transcutaneous transformer,"*IEEE Trans. Power Electron.*, vol. 13, no. 6, pp. 1013_1022,Nov. 1998.
[30] T. Bieler, M. Perrottet, V. Nguyen, and Y. Perriard, ``Contactless powerand information transmission," in *Proc. IEEE-IAS Annu. Meeting Conf.Rec.*, vol. 1, Sep./Oct. 2001, pp. 83_88.
[31] H. Sakamoto, K. Harada, S. Washimiya, K. Takehara, Y. Matsuo, andF. Nakao, ``Large air-gap coupler for inductive charger [for electric
vehicles]," *IEEE Trans. Magn.*, vol. 35, no. 5, pp. 3526_3528, Sep. 1999.
[32] J. Lukacs, M. Kiss, I. Nagy, G. Gonter, R. Hadik, K. Kaszap, andA. Tarsoly, ``Inductive energy collection for electric vehicles," in *Proc.
4th Power Electron.Conf.*, Budapest, Hungary, 1981, pp. 71_81.
[33] K. Lashkari, S. E. Schladover, and E. H. Lechner, ``Inductive powertransfer to an electric vehicle," in *Proc. 8th Int. Vehicle Symp.*, 1986,
pp. 258_267.
[34] J. M. Barnard, J. A. Ferreira, and J. D. van Wyk, ``Sliding transformersfor linear contactless power delivery," *IEEE Trans. Ind. Electron.*, vol. 44,no. 6, pp. 774_779, Dec. 1997.
[35] H. Abe, H. Sakamoto, and K. Harada, ``A noncontact charger using aresonant converter with parallel capacitor of the secondary coil," *IEEE
Trans. Ind. Appl.*, vol. 36, no. 2, pp. 444_451, Mar. 2000.
[36] A. Kawamura, K. Ishioka, and J. Hirai, ``Wireless transmission of powerand information through one high frequency resonant AC link inverterfor robot manipulator applications," in *Proc. 13th IEEE Ind. Appl. Conf.Meeting Conf. Rec. (IAS)*, vol. 3, Oct. 1995, pp. 2367_2372.